Kinetic Studies on the 1,2-Sigmatropic Hydrogen Shift in the Photorearranged Intermediate of *N*-Acetylpyrrole: Tunneling Effects[1]

Yukihiro Kimura, Masataka Yamamoto, Seiji Tobita, and Haruo Shizuka*

Department of Chemistry, Gunma University, Kiryu, Gunma 376, Japan

Received: June 18, 1996; In Final Form: September 10, 1996[⊗]

The rates for the 1,2-sigmatropic hydrogen and deuterium shifts in the ground state of the photorearranged intermediate of *N*-acetylpyrrole were directly measured by means of laser flash photolysis in several solvents; (e.g., 0.27 s^{-1} for 1,2-H shift and 0.12 s^{-1} for 1,2-D shift in nonpolar methylcyclohexane (MCH) at 293 K). The rate of the 1,2-hydrogen shift was remarkably increased by a basic catalyst, such as triethylamine, alcohols, and water. From the experimental results of temperature and isotope effects, it was shown that the 1,2-sigmatropic hydrogen (or deuterium) shift in MCH proceeds via quantum mechanical tunneling processes at two vibrational energy levels: $E = 0$ ($v = v_0$) and $E = E_v$ (=2.9 kcal mol^{-1} for the hydrogen shift or 3.3 kcal mol^{-1} for the deuterium shift) ($v = v_1$) under experimental conditions. The theoretical considerations for the tunneling mechanism were made by use of the tunnel effect theory proposed by Formosinho. The rates obtained by theoretical calculations were in good agreement with experimental ones. It is noteworthy that the 1,2-sigmatropic hydrogen (or deuterium) shift takes place via the intramolecular process at a low concentration of *N*-acetylpyrrole (1.7×10^{-4} M) in dehydrated MCH.

Introduction

Hydrogen atom transfer is one of the most elementary processes both in chemistry and biochemistry. The sigmatropic hydrogen shift is of particular interest from the viewpoint of the Woodward−Hoffmann rule.[2,3] A number of theoretical[4−8] and experimental[9−16] studies on the intramolecular hydrogen shifts both in the ground and excited states have been reported. For the 1,2-sigmatropic hydrogen shift, it is known that singlet carbenes such as benzylchlorocarbene, alkylchlorocarbene, and dialkylcarbene undergo intramolecular hydrogen shifts.[17−28] However, little attention to the detailed mechanistic features of the sigmatropic hydrogen shifts has been given until recently. In a previous paper,[29] we reported that (1) the rate of 1,3-hydrogen shift in the ground state of the photorearranged intermediate of phenyl acetate is greater than that of the 1,5-hydrogen shift, contrary to the prediction of the Woodward−Hoffmann rule,[2,3] showing that the heteroatom of the corresponding carbonyl oxygen plays an important role in the intramolecular hydrogen shift, and (2) the 1,3-sigmatropic hydrogen shift proceeds via tunneling processes from the two discrete vibrational energy levels at $v = v_0$ and $v = v_1$ according to the Boltzmann distribution law.

N-Acetylpyrrole (NAH) isomerizes to 2-acetylpyrrole (2AP) upon irradiation at 254 nm.[30] It has been shown that (1) the photorearrangement of NAH occurs from the lowest excited singlet state S_1 to form the photorearranged intermediate (PRI) by the rearrangement of the acetyl group from the nitrogen atom to the 2-position of the pyrrole ring as shown in eq 1; (2) the quantum yields for the formation of 2AP from NAH in cyclohexane, ethanol, and water at 254 nm at 293 K are known to be 0.53, 0.37, and 0.07, respectively; and (3) no predissociation of the N−C bond resulting in the formation of acetyl and pyrrolyl radicals is involved in the photochemical reaction of NAH. This sigmatropic hydrogen shift looks like a 1,5-sigmatropic shift rather than a 1,2 one according to the Woodward−Hoffmann rule.[2,3] However, this shift is the 1,2-sigmatropic hydrogen shift for the photorearranged intermediate, since the Woodward−Hoffmann rule is applicable for sigmatropic shifts of the carbon framework in which orbital interactions play a dominant role.

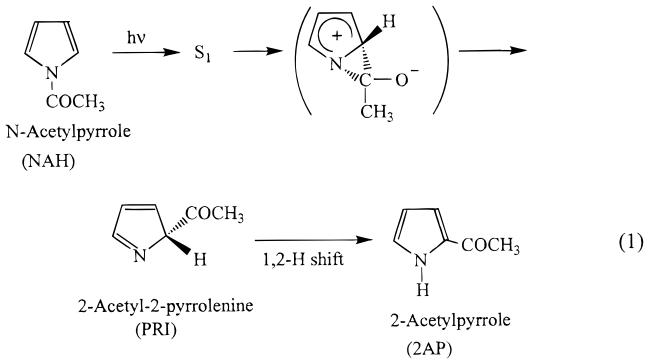

(1)

In the present paper, the isotope and temperature effects on the 1,2-sigmatropic shift of PRI (2-acetyl-2-pyrrolenine) of NAH were studied by 266-nm laser flash photolysis, and theoretical considerations were made according to the tunnel effect theory proposed by Formosinho[31−36] in order to clarify the reaction mechanism.

Experimental Section

N-Acetylpyrrole was prepared by the reaction of pyrrole (Tokyo Kasei guaranteed reagent) with *N*-acetylimidazole (Tokyo Kasei extra pure) according to the procedure reported.[37] The crude was purified by vacuum distillation. Pyrrole-d_5 (Aldrich) and *N*-acetylimidazole-d_3, prepared by the reaction of imidazole (Wako) with acetic-d_6 anhydride (Aldrich), were used for the synthesis of *N*-acetylpyrrole-d_7 (NAD). The crude obtained was purified by column chromatography on silica gel. Deuteration of hydrogen atoms on the pyrrole ring was checked by NMR and mass spectra. Methylcyclohexane (MCH; Aldrich spectrophotometric grade) was dried with molecular sieves 4A, then purified by refluxing over lithium aluminum hydride for 5 h, and finally distilled. Cyclohexane (CH; Aldrich spectropho-

[⊗] Abstract published in *Advance ACS Abstracts,* December 15, 1996.

S1089-5639(96)01797-5 CCC: $14.00

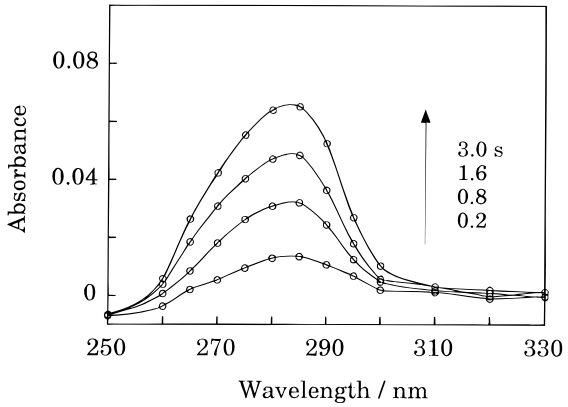

Figure 1. Transient absorption spectra obtained by 266-nm laser flash photolysis of NAH (2.8×10^{-4} M) in CH at 293 K.

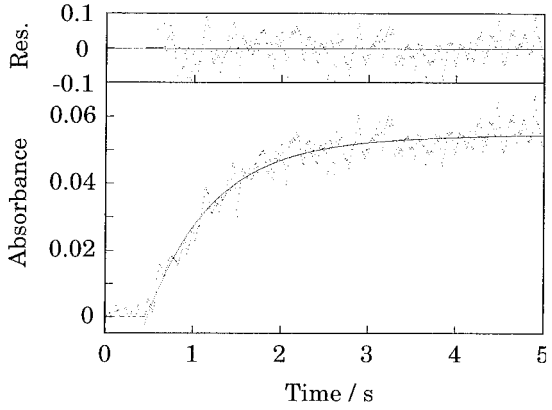

Figure 2. Time trace of transient absorption spectra obtained by 266-nm laser flash photolysis of NAH in MCH monitored at 290 nm.

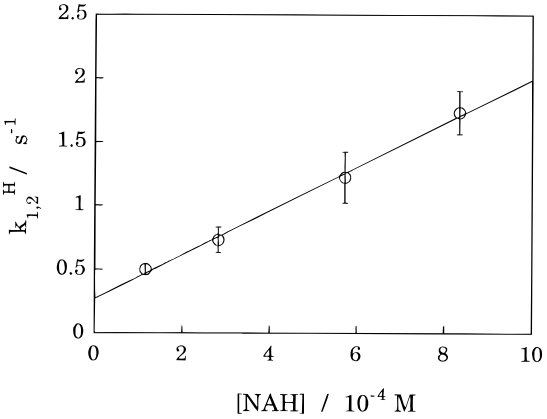

Figure 3. Plots of the observed rates $k_{1,2}^{H}$ in dehydrated MCH as a function of [NAH].

tometric grade), acetonitrile (ACN; Kishida spectrosol), methanol (MeOH; Wako spectrosol), ethanol (EtOH; Wako spectrosol), and propanol (PrOH; Wako spectrosol) were purified by fractional distillations. Triethylamine (TEA; Wako special grade) was purified by vacuum distillation. 2,2,2-Trifluoroethanol (TFE; Wako special grade) was used as received. The kinetic measurements were carried out at a low concentration of NAH (1.7×10^{-4} M) in MCH.

The fourth harmonic (266 nm) of a nanosecond Nd^{3+}:YAG laser (Spectra-Physics GCR-130, pulse width 4−5 ns) was used for excitation. The monitoring system consisted of a 500-W xenon lamp (USHIO, UXL-500D), a monochromator (JOBIN YVON HR320), and a photomultiplier (Hamamatsu, R928). The transient signals were recorded on a digitizing oscilloscope (Tektronix, TDS-540) and transferred to a personal computer (NEC PC-9801 BX3). The kinetic data analysis was made by use of nonlinear least-squares fitting programs.[38]

To avoid the accumulation of photochemical products, fresh samples were used for each laser photolysis. The kinetic measurements were carried out by using a 1-cm or 1-mm quartz cell. The 1-mm cell was used in order to prevent the effect of diffusion on the rise rate. It was confirmed that the effect of dissolved oxygen on the rates for the hydrogen and deuterium shifts was negligible. Therefore, the usual experiments were carried out under aerated conditions. For temperature and concentration effects in nonpolar solvents, the samples were prepared in a drybox filled with nitrogen gas. Molecular orbital calculations were performed at the Hartree−Fock/3-21G level by using the GAUSSIAN 94 program.[39]

Results and Discussion

Intramolecular 1,2-Hydrogen Shift in the Photorearranged Intermediate of *N*-Acetylpyrrole. The steady-state photolysis of NAH has been reported previously.[30] The rate for the 1,2-hydrogen shift of the photorearranged intermediate (PRI) of NAH was directly measured by laser photolysis in cyclohexane (CH) at 293 K. Figure 1 shows the transient absorption spectra obtained by 266-nm laser flash photolysis of NAH (2.82×10^{-4} M) in CH at 293 K. With a lapse of time, an absorption peak around 285 nm appeared. This peak is ascribable to the absorption of photoproduct (2AP) because the shape and the position of this transient spectra are in good agreement with those of 2AP.[30] The formation rate of 2AP corresponding to the rate of the 1,2-hydrogen shift can be determined by measuring the rise time at 290 nm. Figure 2 shows a typical time trace monitored at 290 nm in CH at 293 K. Since the spectral overlap between the photoproduct (2AP) and intermediate (PRI) at 290 nm is negligible, the time trace can be analyzed by the following equation

$$A_{1,2}(t) = A(1 - \exp(-k_{1,2}t)) \qquad (2)$$

where $A_{1,2}(t)$ is the observed time-dependent absorbance at 290 nm, A is the final absorbance, and $k_{1,2}$ is the rise rate of 2AP.

To confirm that the observed rate of the 1,2-hydrogen shift corresponds to the intramolecular process, the concentration effect of the starting material (NAH) on the formation rate of 2AP was examined. Figure 3 shows the plots of the observed formation rates of 2AP as a function of [NAH] in the concentration range $(1.2-8.3) \times 10^{-4}$ M in methylcyclohexane (MCH) at 293 K. The dependence of the formation rate $k_{1,2}^{H}$ on [NAH] indicates that the intermolecular reaction of PRI with NAH is involved in addition to the intramolecular hydrogen shift. Thus, the observed rate $k_{1,2}^{H}$ for the 1,2-hydrogen shift can be expressed as

$$k_{1,2}^{H} = (k_{1,2}^{H})_0 + (k_{1,2}^{H})_{se}[\mathrm{NAH}] \qquad (3)$$

where $(k_{1,2}^{H})_0$ denotes the intrinsic rate constant for the 1,2-hydrogen shift and $(k_{1,2}^{H})_{se}$ stands for the bimolecular rate constant of the self-enhanced 1,2-hydrogen shift by the starting material (NAH). The values of $(k_{1,2}^{H})_0$ and $(k_{1,2}^{H})_{se}$ at 293 K were determined as $2.7(\pm 0.5) \times 10^{-1}$ s^{-1} and $1.7(\pm 0.3) \times 10^{3}$ M^{-1} s^{-1}, respectively. In order to obtain the intrinsic rate constant for the 1,2-hydrogen shift, the concentration of NAH should be as low as possible. Thus, the kinetic measurements were performed at [NAH] = 1.7×10^{-4} M. Moreover, to clarify the effect of the concentration of PRI on $k_{1,2}^{H}$, the laser power dependence was examined (up to 40 mJ $pulse^{-1}$ cm^{-2}). It was confirmed that the effect of laser intensity on $k_{1,2}^{H}$ was

TABLE 1: Rate Constants $(k_{1,2}^{H})_0$ and $(k_{1,2}^{D})_0$ of the 1,2-Sigmatropic Hydrogen and Deuterium Shifts of the Photorearranged Intermediates of NAH and NAD in Various Solvents at 293 K

	solvent	ϵ^a	$(k_{1,2}^{H})_0/s^{-1}$	$(k_{1,2}^{H})_{se}/M^{-1}\ s^{-1}$	$(k_{1,2}^{D})_0/s^{-1}$	$(k_{1,2}^{D})_{se}/M^{-1}\ s^{-1}$
NAH	MCH	2.0	$2.7(\pm0.5) \times 10^{-1}$	$1.7(\pm0.3) \times 10^{3}$		
	CH_3CN	37.5	$1.5(\pm0.4)$	*b*		
	CH_3OH	32.7	$2.5(\pm0.2) \times 10^{3}$	*b*		
	CH_3CH_2OH	24.5	$3.8(\pm0.2) \times 10^{3}$	*b*		
	PrOH	20.3	$4.2(\pm0.4) \times 10^{3}$	*b*		
	H_2O	78.4	$2.6(\pm0.4) \times 10^{4}$	*b*		
	CF_3CH_2OH	26.7	$2.8(\pm0.6) \times 10$	*b*		
NAD	MCH	2.0			$1.2(\pm0.3) \times 10^{-1}$	$4.5(\pm0.7) \times 10^{2}$
	CH_3CN	37.5			$9.5(\pm0.5) \times 10^{-1}$	*b*

[a] Dielectric constants of solvents. From: Isaacs, N. S. *Physical Organic Chemistry*; Wiley: New York, 1987; p 180. [b] There was no self-enhancement effect on the 1,2-hydrogen shift in polar solvents.

scarcely recognized, showing that $k_{1,2}^{H}$ was nearly independent of the concentration of PRI under the experimental conditions.

Solvent Effects on the 1,2-Sigmatropic Hydrogen and Deuterium Shifts. The solvent effects on the 1,2-sigmatropic hydrogen and deuterium shifts were examined in various solvents. Similar transient absorption spectra to those in CH were obtained by 266-nm laser flash photolysis of NAH in polar acetonitrile (ACN) at 293 K. The formation rate ($1.5(\pm0.4)$ s^{-1}) of 2AP in ACN was greater than that in MCH, and there was no self-enhancement effect on $k_{1,2}^{H}$. The rates of the 1,2-sigmatropic hydrogen shift obtained in various solvents are listed in Table 1. From Table 1, it can be seen that the rise rates in protic solvents (e.g., 3.8×10^3 s^{-1} in ethanol and 2.6×10^4 s^{-1} in water) are remarkably fast in comparison with those in aprotic solvents (0.27 s^{-1} in MCH and 1.5 s^{-1} in ACN). This fact suggests that the intermolecular interaction between PRI and alcohol (or water) molecule(s) enhances the rate of the 1,2-hydrogen shift. The self-enhanced hydrogen shift by NAH in alcohols and water was negligible because the formation rates of 2AP in protic solvents were drastically faster than that of the self-enhanced hydrogen shift. To elucidate the significant increase of $k_{1,2}^{H}$ in alcohols and water, the concentration effects of an acidic catalyst such as trifluoroethanol (TFE) and a basic catalyst such as triethylamine (TEA) on $k_{1,2}^{H}$ were examined. Figure 4a shows the plots of the formation rates of 2AP in MCH ([NAH] $= 1.7 \times 10^{-4}$ M) as a function of added TFE concentration. The rate of the 1,2-hydrogen shift can be expressed by

$$k_{1,2}^{H} = (k_{1,2}^{MCH})_0 + (k_{1,2}^{TFE})_e[TFE] \qquad (4)$$

where $(k_{1,2}^{MCH})_0$ and $(k_{1,2}^{TFE})_e$ are the rate constant for 1,2-hydrogen shift in MCH and that due to intermolecular interactions between PRI and TFE, respectively. The bimolecular rate constant for the TFE-catalyzed hydrogen transfer was obtained to be 1.7×10^2 M^{-1} s^{-1} from the slope of the straight line in Figure 4a.

The measurements of $k_{1,2}^{H}$ were also carried out in neat alcohols (methanol, ethanol, and propanol). The results are listed in Table 1. The rate constant of the 1,2-hydrogen shift in TFE is significantly small compared with those in alcohols as shown in Table 1, and there exists the tendency that the more the basicity of the oxygen atom of the alcohol molecule increases, the more the rate of 1,2-hydrogen shift becomes large. That is, the basicity of catalyst may play an important role. The effect of TEA on the rate of 1,2-hydrogen shift in nonpolar CH ([NAH] $= 1.7 \times 10^{4}$ M) at 293 K was examined. The plots of the formation rates as a function of [TEA] are shown in Figure 4b. The basic catalytic effect of TEA in CH can be expressed

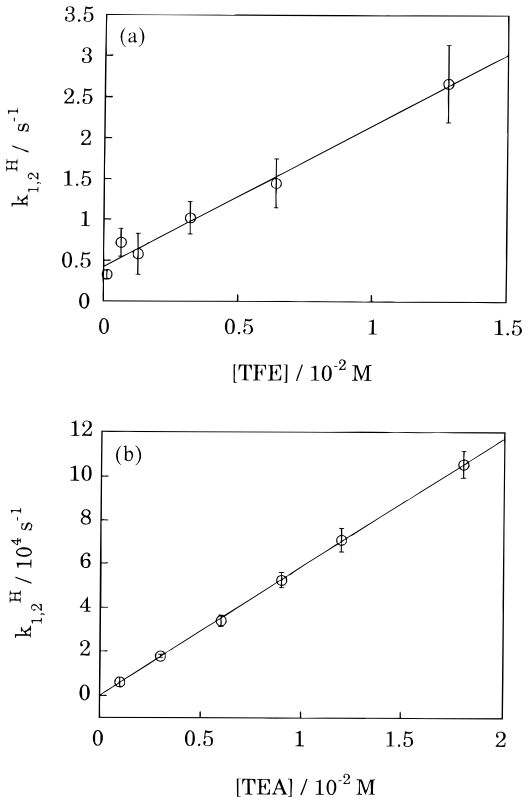

Figure 4. Plots of the observed formation rates of 2AP from NAH in MCH as a function of [TFE] (a) and that in CH as a function of [TEA] (b).

by the following equation:

$$k_{1,2}^{H} = (k_{1,2}^{CH})_0 + (k_{1,2}^{TEA})_e[TEA] \qquad (5)$$

where $(k_{1,2}^{CH})_0$ and $(k_{1,2}^{TEA})_e$ denote the rate constants for the 1,2-hydrogen shift in CH at [NAH] $= 1.7 \times 10^{-4}$ M and for the intermolecular hydrogen shift enhanced by TEA, respectively. The value of $(k_{1,2}^{TEA})_e$ was obtained as 5.9×10^6 M^{-1} s^{-1}. This result shows that the intermolecular 1,2-hydrogen atom transfer is enhanced by the basic catalyst TEA. That is, the proton exchange reaction between PRI and TEA takes place as shown in eq 6. It is known that similar basic catalysis occurs in the case of the 1,3- and 1,5-hydrogen shifts of the photorearranged intermediates of phenyl acetate.[29] It can be said that the mechanism of catalytic effects of TEA, alcohols, and water on the 1,2-hydrogen shift is due to the basic catalysis.

It is noteworthy here that the 1,2-sigmatropic hydrogen shift proceeds via intramolecular process in dehydrated MCH at a low concentration of NAH (1.7×10^{-4} M).

Isotope Effect on the 1,2-Sigmatropic Hydrogen Shift. The isotope effect on the 1,2-sigmatropic hydrogen shift was

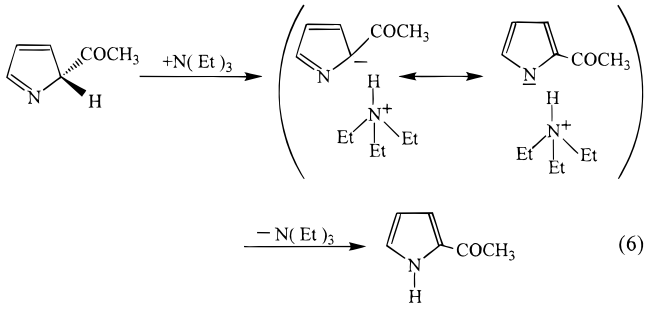

(6)

examined by use of *N*-acetylpyrrole-d_7 (NAD). The transient absorption spectra were obtained by 266-nm laser flash photolysis of NAD (2.8×10^{-4} M) in MCH at 293 K. The spectra were similar to those of NAH. The rate $k_{1,2}{}^{D}$ of the 1,2-deuterium shift can be given by

$$k_{1,2}{}^{D} = (k_{1,2}{}^{D})_0 + (k_{1,2}{}^{D})_{se}[\mathrm{NAD}] \qquad (7)$$

where $(k_{1,2}{}^{D})_0$ and $(k_{1,2}{}^{D})_{se}$ are the intrinsic rate constant for the 1,2-sigmatropic deuterium shift and the self-enhanced rate constant for the 1,2-deuterium shift by the starting material (NAD), respectively. The rate constants $(k_{1,2}{}^{D})_0$ and $(k_{1,2}{}^{D})_{se}$ at 293 K were obtained to be $1.2(\pm 0.3) \times 10^{-1}$ s^{-1} and $4.5(\pm 0.7) \times 10^2$ M^{-1} s^{-1}, respectively. The kinetic isotope effect of $(k_{1,2}{}^{H})_0/(k_{1,2}{}^{D})_0$ was obtained as 2.3 at 293 K. The isotope effect increases with decreasing temperature up to ca. 12, as will be described in the next section.

The basic catalysis effect on the 1,2-deuterium shift was also examined. The rates of the 1,2-deuterium shift were measured in various concentrations of TEA at $[\mathrm{NAD}] = 1.7 \times 10^{-4}$ M in MCH. From similar treatments to the case of NAH, the value of $(k_{1,2}{}^{TEA})_e$ for the 1,2-deuterium shift in MCH was obtained to be 1.2×10^6 M^{-1} s^{-1} within 15% error.

Temperature Effects on the 1,2-Sigmatropic Hydrogen Shift. The measurements of the temperature effect on the 1,2-sigmatropic hydrogen (or deuterium) shift of the PRI produced by 266-nm laser flash photolysis were carried out at a low concentration of NAH or NAD (1.7×10^{-4} M) in dehydrated MCH to avoid the intermolecular reactions with the starting material (NAH or NAD) or a trace of water in MCH. Figure 5 shows the plots of the observed rates $k_{1,2}$ ($k_{1,2}{}^{H}$ or $k_{1,2}{}^{D}$) as a function of T^{-1} in dehydrated MCH. The Arrhenius plots give a straight line in the high-temperature range ≥ ca. 250 K. However, the slope of the plots gradually becomes small in the low-temperature range ≤ ca. 250 K. This fact indicates that 1,2-sigmatropic hydrogen and deuterium shifts probably proceed via the quantum mechanical tunneling in the electronically ground state.

Most of the tunnel corrections have been made by the concept of a continuous Boltzmann distribution of energies.[40] However, the energy of molecular vibrations is certainly quantized and the separation of the vibrational levels is much greater than $k_B T$ for the range of temperatures normally encountered. Particularly, in the intramolecular proton or hydrogen atom transfer, there is no contribution from translational kinetic energy and the assumption of a continuous energy distribution appears less reasonable. It is suggested that tunneling from one or more discrete levels is a more appropriate model than that of a continuous energy distribution.[40] In fact, the formation rates of $k_{1,2}{}^{H}$ and $k_{1,2}{}^{D}$ for NAH and NAD, respectively, can be expressed by eq 8, taking the Boltzmann distribution at T (K)

$$k_{1,2} = \frac{k_1 + k_2 \exp(-\Delta E/RT)}{1 + \exp(-\Delta E/RT)} \qquad (8)$$

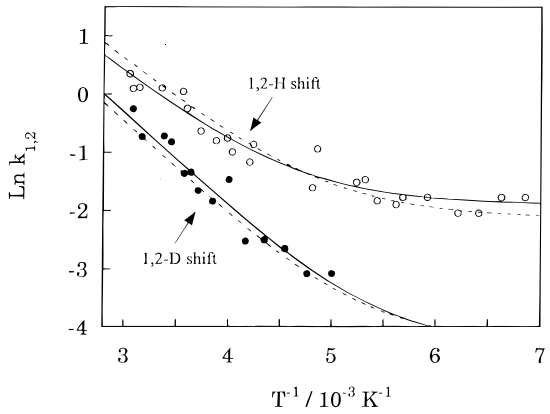

Figure 5. Arrhenius plots of the observed rates for the 1,2-sigmatropic hydrogen (open circle) and deuterium (closed circle) shifts of NAH and NAD in MCH. Broken lines denote the calculated rates. For details, see text.

between two discrete vibrational energy levels ($v = v_0$ and $v = v_1$) into account, where ΔE is the energy difference between the two vibrational levels ($v = v_0$ and $v = v_1$) and k_1 and k_2 are their temperature-independent reaction rate constants, as will be described later. By the best fit of eq 8 to the plots of ln $k_{1,2}$ vs T^{-1} in Figure 5, the values of $k_1{}^{H}$, $k_2{}^{H}$, and ΔE^{H} were determined to be 0.15 s^{-1}, 1.1×10^2 s^{-1}, and 2.9 kcal mol^{-1} ($=1.0 \times 10^3$ cm^{-1}) for the 1,2-hydrogen shift of NAH, respectively. Similarly, the values of $k_1{}^{D}$, $k_2{}^{D}$, and ΔE^{D} were determined as 1.3×10^{-2} s^{-1}, 1.0×10^2 s^{-1}, and 3.3 kcal mol^{-1} ($=1.2 \times 10^3$ cm^{-1}) for the 1,2-deuterium shift of NAD, respectively. These data are summarized in Table 2. The best fitted values of $k_{1,2}$ are shown by the solid lines in Figure 5. The experimental results for both temperature and isotope effects on $k_{1,2}$ strongly support the quantum mechanical tunneling for the 1,2-sigmatropic hydrogen and deuterium shifts.

Theoretical Consideration for the 1,2-Sigmatropic Hydrogen Shift via Tunneling. To confirm the quantum mechanical tunneling mechanism for the 1,2-sigmatropic hydrogen shift of the PRI of NAH, theoretical considerations were made. Theoretical methods for the hydrogen atom transfer via tunneling have been extensively developed by Formosinho.[31−36] The potential energy surfaces both for PRI and the final product (2AP) for the 1,2-hydrogen shift were calculated by his method. In the reactant system, the force constant f_r was estimated by use of the C═N and C−H force constants ($f_{C=N}$ and f_{C-H}) for C═N and C−H stretching vibrations in PRI as follows:[31−33]

$$f_r^2 = f_{C=N}{}^2 + f_{C-H}{}^2 + 2 f_{C=N} f_{C-H} \cos\theta(\mathrm{C{=}N,\ C{-}H}) \qquad (9)$$

The value of f_r for the C═N and C−H system (or the C═N and C−D system) was obtained as 6.30×10^7 cm^{-1} nm^{-2} (or 6.02×10^7 cm^{-1} nm^{-2}). The harmonic potential V_r for PRI is given by

$$V_r = \frac{1}{2} f_r x^2 \qquad (10)$$

where x is the reaction coordinate, i.e., the common displacement of the C═N and C−H bonds. Zero-point vibrational energies can be neglected, because the total zero-point energy of a polyatomic molecule is spent in motions in directions irrelevant for the reaction coordinates.[32]

In the product (2AP) system, the force constant f_P was also estimated by using the force constants f_{C-N} and f_{N-H} of the C−N

TABLE 2: Rate Constants and Parameters for 1,2-Hydrogen and Deuterium Shifts via Tunneling[a]

	1,2-hydrogen shift				1,2-deuterium shift			
	exptl		theoretical		exptl		theoretical	
	$v = 0$	$v = v_1$	$v = 0$	$v = v_1$	$v = 0$	$v = v_1$	$v = 0$	$v = v_1$
$f_r/10^7$ cm^{-1} nm^{-2}			6.30	6.30			6.02	6.02
$f'_p/10^7$ cm^{-1} nm^{-2}			3.95	3.95			3.92	3.92
$\Delta R/10^{-2}$ nm			5.09	5.09			5.09	5.09
$\Delta x/10^{-2}$ nm			2.96				2.95	
$\Delta x'/10^{-2}$ nm				2.28				2.18
$E_B/10^4$ cm^{-1}			1.12	1.12			1.09	1.09
$E_v/10^3$ cm^{-1}	0	1.0	0	1.0	0	1.2	0	1.2
$\mu/10^{-26}$ kg			2.04[b]	2.04[b]			2.46[b]	2.46[b]
k_1/s^{-1}	0.15		0.12		1.3×10^{-2}		1.4×10^{-2}	
k_2/s^{-1}		1.1×10^2		1.4×10^2		1.0×10^2		0.9×10^2

[a] For details, see text. [b] Calculated by use of eq 17.

and N−H stretching vibrations in 2AP.[31−33]

$$f_P^2 = f_{C-N}^2 + f_{N-H}^2 - 2f_{C-N}f_{N-H}\cos\theta(\text{C}-\text{N, N}-\text{H}) \quad (11)$$

The negative sign arises because the two oscillators vibrate out of phase, immediately after the hydrogen atom transfer. Since the motions of all the atoms are not independent, e.g.,

$$x_{NH} = -(x_{CN} + x_{CH}) \quad (12)$$

all the vibrations can be considered along a common bond-stretch direction. By projecting the stretching motion of the N−H bond in the system of axes of PRI, eq 13 can be derived:[31−33]

$$f'^2_P = f_{C-N}^2 + f'^2_{N-H} - 2f_{C-N}f'_{N-H}\cos\theta(\text{C}=\text{N, C}-\text{H}) \quad (13)$$

where $f'_{N-H} = f_{N-H}[\cos\theta\,(\text{CN, NH}) + \cos\theta\,(\text{CH, NH})]$. The values of f'_P for the hydrogen- and the deuterium-shifted products were obtained to be 3.95×10^7 and 3.92×10^7 cm^{-1} nm^{-2}, respectively. The angle of the three displacement coordinate axes is taken as the angle, θ, of the coordinate axes for a triatomic molecule *XYZ* with atomic masses m_1, m_2, and m_3:

$$\cos\theta = \left[\frac{m_1 m_3}{(m_1 + m_2)(m_2 + m_3)}\right]^{1/2} \quad (14)$$

The angle between $x_{C=N}$ and x_{C-H} of PRI can be estimated with $m_1 = 1$, $m_2 = 24$, and $m_3 = 14$, where m_2 concentrates the mass of the two carbon atoms.

Parts a and b of Figure 6 show the calculated potential energy diagrams for the 1,2-hydrogen and deuterium shifts, where V_r and V_p denote the potential surfaces of the photorearranged intermediate and photoproduct, respectively, ΔH denoted the enthalpy change for the 1,2-hydrogen shift obtained by the ab initio calculations (see below), ΔR denotes the coordinate displacement, E_B denotes the energy of crossing of the potential curves, E_v denotes the vibrational energy for v_1 (i.e., $E_v = \Delta E$), and Δx and $\Delta x'$ denote the distances between the potential curves of the initial and final states at $E = 0$ and $E = E_v$, respectively. Figure 6 can be used for the theoretical considerations according to the tunnel effect theory.[34]

The energy diagram for the photorearrangement of NAH calculated by the ab initio MO method to estimate the value of ΔH is shown in Figure 7. The value of ΔH for the 1,2-hydrogen shift in PRI was estimated to be −25.67 kcal mol^{-1} from the ab initio calculations. This result shows that the 1,2-hydrogen

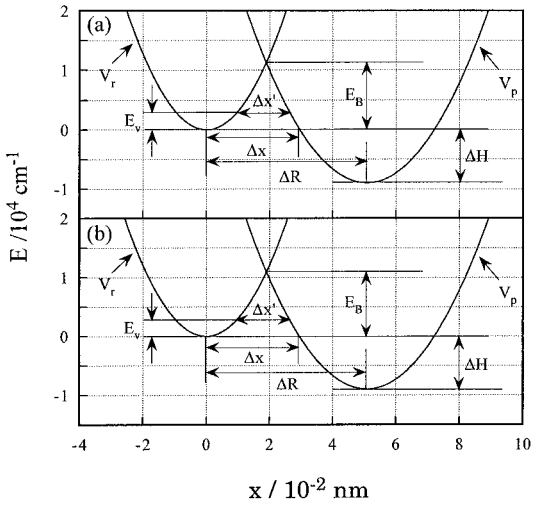

Figure 6. Potential energy curves of C═N and C−H (or C−D) oscillators in the photorearranged intermediate (PRI) and C−N and N−H (or N−D) oscillators in 2AP for the 1,2-hydrogen and -deuterium shifts of NAH (a) and NAD (b).

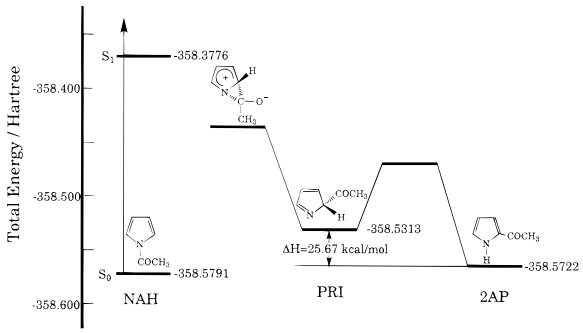

Figure 7. Energy profile for the 1,2-sigmatropic hydrogen shift in the photorearranged intermediate of NAH calculated by the ab initio method (3-21G).

shift in the present system is an exothermic reaction. As a result, the potential energy of 2AP is given by the following equation:

$$V_P = \frac{1}{2}f'_P(x - \Delta R)^2 + \Delta H \quad (15)$$

The values of E_B and Δx for the 1,2-sigmatropic hydrogen shift in Figure 6 were determined as 1.12×10^4 cm^{-1} (32.02 kcal mol^{-1}) and 2.96×10^{-2} nm, respectively. Because of the large energy barrier E_B, the hydrogen shift does not take place beyond the energy barrier under the experimental conditions. The values of E_B and Δx for the 1,2-sigmatropic deuterium shift were obtained to be 1.09×10^4 cm^{-1} (31.16 kcal mol^{-1}) and 2.95×10^{-2} nm, respectively. According to the tunnel effect

theory,[34, 40] the tunneling rate k can be calculated by use of the values E_B and Δx

$$k = \nu \exp\left\{-\frac{2\pi}{h}[2\mu(E_B - E_V)]^{1/2}\Delta x\right\} \quad (16)$$

where $k = k_1$ at $v = v_0$ (i.e., $E_v = 0$, $\Delta x = \Delta x$) and $k = k_2$ at $v = v_1$ (i.e., $E_v = \Delta E$, $\Delta x = \Delta x'$). Here, ν is the average frequency for the tunneling and generally taken as 10^{13} s^{-1} in the case of intramolecular reaction.[40] However, in the present system, the frequency is very small since the reaction occurs only when all the corresponding oscillators vibrate as promoting modes. Therefore, the frequency of the tunneling reaction was obtained to be 5×10^{10} s^{-1} by the best fitting method with use of eqs 8 and 16.

The value of E_v in eq 16 is equal to the energy difference ΔE between two discrete vibrational levels as stated above. Here, μ is the reduced mass estimated by[31,32]

$$\mu^{1/2} = \mu_{CN}^{1/2} + \mu_{CH}^{1/2} \quad (17)$$

where μ_{CN} and μ_{CH} are the reduced masses for the CN and CH vibrations.

The value of ΔR (the displacement between the potential minima of reactant and product along with the reaction coordinate) was calculated by means of the intersecting-state model (ISM) proposed by Formosinho.[32,36] According to the ISM model, the sum of the bond distensions, d, at the transition state is expressed as

$$d = \frac{a' \ln 2}{n^{\ddagger}}(r_p + r_r) \quad (18)$$

where a' is a constant (=0.156), r_p and r_r are the equilibrium bond lengths of product and reactant, respectively, and $n^{\ddagger}$ is the bond order at the transition state. In the present system, two kinds of bond rearrangements are involved, e.g., H (from C—H to N—H) and N (from C═N to C—N). In the first place, for the bond rearrangement of H-migration which includes the processes of C—H bond-breaking and N—H bond-forming, the transition-state bond order $n^{\ddagger}$ is 0.5. Therefore,

$$d_{XH} = \frac{a' \ln 2}{0.5}(r_{C-H} + r_{N-H}) \quad (19)$$

is derived.

In the second place, for the CN rearrangement involving a bond-breaking process from C═N to C—N, the transition bond order also equals 0.5. Thus,

$$d_{CN} = \frac{a' \ln 2}{0.5}(r_{C=N} + r_{C-N}) \quad (20)$$

The value of the bond distension ($d = \Delta R$) is represented by eq 21 as the average of the two bond distensions d_{XH} (X = C or N) for H and d_{CN} for N. The optimized bond lengths are

$$\Delta R = \frac{1}{2}(d_{XH} + d_{CN}) \quad (21)$$

obtained as $r_{C-H} = 10.87 \times 10^{-2}$ nm, $r_{N-H} = 9.95 \times 10^{-2}$ nm, $r_{C=N} = 12.73 \times 10^{-2}$ nm, and $r_{C-N} = 13.65 \times 10^{-2}$ nm by ab initio MO calculations. By substituting these values for r_{CH}, r_{NH}, $r_{C=N}$, and r_{C-N} into eqs 19 and 20, the values of d_{XH} and d_{CN} are obtained as 4.50×10^{-2} and 5.71×10^{-2} nm, respectively, and ΔR is determined to be 5.09×10^{-2} nm.

The values of $\Delta x'$ at $E = E_v$ (=ΔE) were calculated from the potential energy curves to be 2.28×10^{-2} nm for the hydrogen shift and 2.18×10^{-2} nm for the deuterium shift. The parameters used to obtain the theoretical tunneling rates are listed in Table 2. By using these tunneling parameters and eq 16, the tunneling rate constants, k_1 and k_2 for the 1,2-hydrogen shift at $v = v_0$ and $v = v_1$, were obtained as 0.12 and 1.4×10^2 s^{-1}, respectively. For the 1,2-deuterium shift, k_1 and k_2 at $v = v_0$ and $v = v_1$ were obtained to be 1.4×10^{-2} and 0.9×10^2 s^{-1}, respectively.

By use of these tunneling rate constants k_1 and k_2, the values of $k_{1,2}$ can be calculated by eq 8 at various temperatures. The $k_{1,2}$ values for the 1,2-hydrogen and deuterium shifts are plotted in Figure 5 (broken lines). The good agreements between the experimental and theoretical values for $k_{1,2}$ show that the 1,2-hydrogen and deuterium shifts proceed via tunneling processes at $v = v_0$ ($E = 0$) and $v = v_1$ ($E = E_v$ (2.9 kcal mol^{-1} for the hydrogen shift and 3.3 kcal mol^{-1} for the deuterium shift)) according to the Boltzmann distribution law.

Concluding Remarks

The following concluding remarks are drawn by the direct measurements of the 1,2-sigmatropic hydrogen (or deuterium) shift of the PRI of *N*-acetylpyrrole and also the theoretical considerations according to the tunnel effect theory proposed by Formosinho.[31−36]

(1) The rates for the 1,2-sigmatropic hydrogen (or deuterium) shift of the PRI of NAH produced by 266-nm laser flash photolysis are directly measured in several solvents. It is found that the rate of the 1,2-hydrogen shift is enhanced by the starting material (NAH or NAD) and the intramolecular rate constant for the 1,2-sigmatropic hydrogen or deuterium shift is determined to be 0.27 s^{-1} for NAH (0.12 s^{-1} for NAD) in MCH at 293 K. It is noteworthy that the 1,2-sigmatropic hydrogen shift proceeds via the intramolecular process at a low concentration of NAH (1.7×10^{-4} M) in dehydrated MCH.

(2) The rate of 1,2-hydrogen shift is remarkably increased by a basic catalyst, such as triethylamine, alcohols, and water. The effect of the basic catalyst on the 1,2-hydrogen shift can be explained by proton exchange between the intermediate (PRI) and the basic catalysts.

(3) On the basis of the experimental and theoretical results of temperature and isotope effects, it is shown that the intramolecular 1,2-hydrogen (or deuterium) shift in MCH proceeds via quantum mechanical tunneling at two vibrational energy levels: $E = 0$ ($v = v_0$) and $E = E_v$ (=2.9 kcal mol^{-1} for the hydrogen shift or 3.3 kcal mol^{-1} for the deuterium shift) ($v = v_1$) under the experimental conditions.

Acknowledgment. This work was supported by a Grant-in-Aid on Priority-Area-Research: Photoreaction Dynamics (06239101) from the Ministry of Education, Science and Culture of Japan. We thank Professor Susumu Tajima of Gunma College of Technology for MS measurements of NAH and NAD.

References and Notes

(1) This work was presented at The International Symposium on Recent Progress and Future Prospects of Molecular Electronic Spectroscopy in honor of Professor Saburo Nagakura, Hayama, Japan, Oct 1995.
(2) Woodward, R. B.; Hoffmann, R. *J. Am. Chem. Soc.* **1965**, *87*, 2511.
(3) Fleming, I. *Frontier Orbitals and Organic Chemical Reactions*; Wiley: New York, 1976.
(4) Evanseck, J. D.; Houk, K. N. *J. Phys. Chem.* **1990**, *94*, 5518.
(5) Dorigo, A. E.; McCarrick, M. A.; Loncharich, R. J.; Houk, K. N. *J. Am. Chem. Soc.* **1990**, *112*, 7508.
(6) Bernardi, F.; Olivucci, M.; Robb, M. A.; Tonachini, G. *J. Am. Chem. Soc.* **1992**, *114*, 5805.
(7) Sobolewski, A. L. *Chem. Phys. Lett.* **1993**, *211*, 293.
(8) Tapia, O.; Andrés, J.; Safont, V. S. *J. Phys. Chem.* **1994**, *98*, 4821.

(9) Duhaime, R. M.; Weedon, A. C. *Can. J. Chem.* **1987**, *65*, 1867.
(10) Grellmann, K. H.; Weller, H.; Tauer, E. *Chem. Phys. Lett.* **1983**, *95*, 195.
(11) Al-Soufi, W.; Grellmann, K. H.; Nickel, B. *J. Phys. Chem.* **1991**, *95*, 10503.
(12) Al-Soufi, W.; Eychmüller, A.; Grellmann, K. H. *J. Phys. Chem.* **1991**, *95*, 2022.
(13) Reid, P. J.; Wickham, S. D.; Mathies, R. A. *J. Phys. Chem.* **1992**, *96*, 5720.
(14) Liu, M. T. H. *Acc. Chem. Res.* **1994**, *27*, 287.
(15) Sekiguchi, T.; Yamaji, M.; Tatemitsu, H.; Sakata, Y.; Shizuka, H. *J. Phys. Chem.* **1993**, *97*, 7003.
(16) (a) Garcia-Garibay, M. A.; Gamarnik, A.; Pang, L.; Jenks, W. S. *J. Am. Chem. Soc.* **1994**, *116*, 12095. (b) Garcia-Garibay, M. A.; Gamarnik, A.; Bise, R.; Pang, L.; Jenks, W. S. *J. Am. Chem. Soc.* **1995**, *117*, 10264.
(17) Friedman, L.; Shechter, H. *J. Am. Chem. Soc.* **1959**, *81*, 5512.
(18) Kirmse, W.; Buschhoff, M. *Chem. Ber.* **1967**, *100*, 1491.
(19) (a) Moritani, I.; Yamamoto, Y.; Murahashi, S. *Tetrahedron Lett.* **1968**, 5697. (b) Moritani, I.; Yamamoto, Y.; Murahashi, S. *Tetrahedron Lett.* **1968**, 5755.
(20) Sohn, M. B.; Jones, M. *J. Am. Chem. Soc.* **1972**, *94*, 8280.
(21) Pomerantz, M.; Witherup, T. H. *J. Am. Chem. Soc.* **1973**, *95*, 5977.
(22) Jackson, J. E.; Soundararajan, N.; Platz, M. S.; Liu, M. T. H. *J. Am. Chem. Soc.* **1988**, *110*, 5595.
(23) Liu, M. T. H.; Bonneau, R. *J. Am. Chem. Soc.* **1992**, *114*, 3604.
(24) Modarelli, D. A.; Morgan, S.; Platz, M. S. *J. Am. Chem. Soc.* **1992**, *114*, 7034.
(25) (a) Moss, R. A.; Ho, G.-J.; Liu, W.; Sierakowski, C. *Tetrahedron Lett.* **1992**, *33*, 4287. (b) Moss, R. A.; Ho, G.-J.; Liu, W.; Sierakowski, C. *Tetrahedron Lett.* **1993**, *34*, 927.
(26) Dix, E. J.; Herman, M. S.; Goodman, J. L. *J. Am. Chem. Soc.* **1993**, *115*, 10424.
(27) Liu, M. T. H.; Bonneau, R.; Wierlacher, S.; Sander, W. *J. Photochem. Photobiol. A. Chem.* **1994**, *84*, 133.
(28) Wierlacher, S.; Sander, W.; Liu, M. T. H. *J. Am. Chem. Soc.* **1993**, *115*, 8943.
(29) (a) Arai, T.; Tobita, S.; Shizuka, H. *J. Am. Chem. Soc.* **1995**, *117*, 3968. (b) Arai, T.; Tobita, S.; Shizuka, H. *Chem. Phys. Lett.* **1994**, *223*, 521.
(30) (a) Shizuka, H.; Okutsu, E.; Mori, Y.; Tanaka, I. *Mol. Photochem.* **1969**, *1*, 135. (b) Shizuka, H.; Ono, S.; Morita, T.; Tanaka, I. *Mol. Photochem.* **1971**, *3*, 203.
(31) Formosinho, S. J. *J. Chem. Soc., Faraday Trans. 2* **1976**, *72*, 1313.
(32) Formosinho, S. J.; Arnaut, L. G. *Advances in Photochemistry*; John Wiley & Sons: New York, 1991; Vol. 16, p 67.
(33) Formosinho, S. J. *Mol. Photochem.* **1976**, *7*, 41.
(34) Formosinho, S. J. *J. Chem. Soc., Faraday Trans. 2* **1974**, *70*, 605.
(35) Formosinho, S. J.; da Silva, J. D. *Mol. Photochem.* **1974**, *6*, 409.
(36) Varandas, A. J. C.; Formosinho, S. J. *J. Chem. Soc., Faraday Trans. 2* **1986**, *82*, 953.
(37) Reddy, G. S. *Chem. Ind.* **1965**, 1426.
(38) Yamaji, M.; Aihara, Y.; Itoh, T.; Tobita, S.; Shizuka, H. *J. Phys. Chem.* **1994**, *98*, 7014.
(39) Gaussian 94, Revision A.1: Frisch, M. J.; Trucks, G. W.; Schlegel, H. B.; Gill, P. M. W.; Johnson, B. G.; Robb, M. A.; Cheeseman, J. R.; Keith, T. A.; Petersson, G. A.; Montgomery, J. A.; Raghavachari, K.; Al-Laham, M. A.; Zakrzewski, V. G.; Ortiz, J. V.; Foresman, J. B.; Cioslowski, J.; Stefanov, B. B.; Nanayakkara, A.; Challacombe, M.; Peng, C. Y.; Ayala, P. Y.; Chen, W.; Wong, M. W.; Andres, J. L.; Replogle, E. S.; Gomperts, R.; Martin, R. L.; Fox, D. J.; Binkley, J. S.; Defrees, D. J.; Baker, J.; Stewart, J. P.; Head-Gordon, M.; Gonzalez, C.; Pople, J. A.; Gaussian, Inc., Pittsburgh, PA, 1995.
(40) Bell, R. P. *The Tunnel Effect in Chemistry*; Chapman and Hall: London, 1980.